

ROBUSTNESS OF MODAL FILTERS USING PIEZOELECTRIC SENSOR ARRAYS SUBJECT TO POSITIONING UNCERTAINTIES

Marcelo A. Trindade, Carlos C. Pagani Jr. and Ernesto Massaroppi Jr.

*Department of Mechanical Engineering, São Carlos School of Engineering, University of São Paulo,
Av. Trabalhador São-Carlense, 400, São Carlos-SP, 13566-590, Brazil*

Keywords: Modal filters, Piezoelectric sensor arrays, Stochastic modeling, Uncertainty analysis.

Abstract. Modal transducers allow independent sensing, actuation and control of individual vibration modes. Shaped piezoelectric layers were initially proposed to this end but an array of independent piezoelectric transducers with weighted actuation/sensing signals were shown to be easier to implement and allows reconfigurable modal filters since the weighting can be done via software. Several methodologies to determine optimal weights for a modal filter based on a given array of sensors were proposed in the literature. In a previous work, a methodology for the topology optimization of piezoelectric sensor arrays in order to maximize the effectiveness of a set of selected modal filters was presented. This was done using a genetic algorithm optimization for the selection of twelve piezoceramic sensors, from an array of thirty-six piezoceramic sensors regularly distributed over an aluminum plate, which maximize the frequency-band of a set of modal filters, each one aiming at one of the first vibration modes. It was shown that it is possible to improve the effectiveness and frequency-band of a set of modal filters with a reduced number of sensors by optimizing the topology of the sensor array. However, this optimization may also lead to a higher sensitivity of modal filters performance on design parameters. Therefore, this work presents a robustness analysis of modal filters using a topology optimized array design with a reduced number of sensors subjected to uncertainties in the weighting coefficients and sensors positioning. For the weighting coefficients uncertainties, this is done using stochastic modeling tools to build a probabilistic model of the uncertain parameters and Monte Carlo method to evaluate the realizations of modal filters performance indices. For the sensors positioning uncertainties, a sampling-based sensitivity analysis was performed. Latin Hypercube Sampling technique was used to reduce the number of samples and alleviate the computational cost of analyzing multiple topologies. It is shown that optimal filter output is less sensitive to weighting coefficients uncertainties and more sensitive to sensors positioning.

1 INTRODUCTION

Smart structures are integrated systems, composed of a host structure, sensors and actuators which are able to monitor and act to ensure both structural integrity and adaptability to changes in operational conditions. The development of materials having special functional properties has made possible the development of new generation of both sensors and actuators. In the concept of modern science, the actuator effect is defined according to the material's capability of generating mechanical energy from electric, magnetic or thermal energy, while the sensor effect, on the other hand, is defined by the converse energy conversion (Chopra, 2002).

The use of piezoelectric materials (specially piezoceramics) as sensing and actuating elements has been extensively studied due to the possibility of building them as lightweight and compact devices in several geometric configurations, since they are relatively inexpensive and present the necessary electromechanical coupling. In terms of applications, integrated piezoelectric sensors and actuators have been most often applied to the active control of mechanical vibration and noise in structures subjected to several types of excitation, or even self-excited structures, especially for aeronautic and aerospace applications (Chopra, 2002).

On the other hand, the performance of integrated systems applied to active vibration and noise control can be substantially improved by the use of high quality modal filters (Chen and Shen, 1997, Sun et al., 2001). In this context, the development of active control strategies with optimal performance using modal sensors and actuators has been the object of intensive research. Modal sensors and actuators working in closed loop enable to observe and control independently specific vibration modes, reducing the apparent dynamical complexity of the system and the necessary energy to control them (Fripp and Atalla, 2001; Preumont et al., 2003; Friswell, 2001). The high performance of modal controllers depends on the several parameters. The size, form and also the quality of piezoelectric material's effective electromechanical coupling coefficient must be considered to the development of modal sensors and actuators. Though pioneer projects have considered the development of continuous modal sensors and actuators, the evolution of modal filter techniques and its applications to active vibration control indicates several advantages in the use of an array of discrete sensors instead (Shelley, 1991).

The high performance of discrete sensors array depends on the convenient weighting of the sensors signals, in order to achieve optimal modal isolation (Fripp and Atalla, 2001; Preumont et al., 2003). Several numerical methods have been used for the evaluation of the weighting coefficients for the signals measured by the array of sensors (Meirovitch and Baruh, 1982; Shelley, 1991; Chen and Shen, 1997). These techniques may lead to high-performance modal filters, but generally within a limited frequency band.

Preumont et al. (2003) have suggested that the frequency band of high-performance filtering depends on the relation between the number of vibration modes to be filtered, in that frequency band, and the number of sensors in the array. They conclude that the number of sensors in the array should be larger than the number of vibration modes to be filtered. Although this is true for an arbitrarily distributed array of sensors, it is possible to show that the location of the sensors, that is the array topology, has a significant effect on the observability of the vibration modes and, thus, on the filtering performance of modal filters derived from it. Therefore, it should be possible to optimize the array topology and, consequently, increase the number of filtered vibration modes, thus the frequency band, for a given number of sensors available.

Topology optimization techniques are common in advanced structural design, for instance the simultaneous design of actuated mechanical devices, and often present a multiobjective character (Frecker, 2003). Techniques for topology optimization include but are not limited

to genetic algorithms search methods. Genetic algorithm (GA) methods are search algorithms based on the survival of the fittest theory applied for a structured set of parameters Goldberg (1989). GA-based optimization methods have also been used for the design optimization of controlled structures (Han and Lee, 1999; Trindade, 2007).

Previous studies focused on designing and validating a methodology for the topology optimization of a sensor array with the objective of improving the performance of modal filters derived from it (Pagani and Trindade, 2008a, 2008b, 2009). This was done combining a standard technique for the evaluation of the coefficients for weighting the sensors signals with a proposed strategy for the optimization of the sensor array topology. The methodology was applied to a free plate with an array of thirty-six bonded piezoceramic patch sensors. A set of modal filters, aiming at isolating the first five vibration modes of the plate, were evaluated using only selected twelve of the thirty-six sensors of the array. An optimization strategy based on GA was proposed to find a sensor array topology that minimizes the norm of the filtering residue along a wider frequency band. It was shown that it is possible to improve the effectiveness and frequency-band of a set of modal filters with a reduced number of sensors by optimizing the topology of the sensor array. However, this optimization may also lead to a higher sensitivity of modal filters performance on design parameters.

Therefore, this work presents a robustness analysis of modal filters using a topology optimized array design with a reduced number of sensors subjected to uncertainties in the weighting coefficients and sensors positioning. For the weighting coefficients uncertainties, this is done using stochastic modeling tools to build a probabilistic model of the uncertain parameters and Monte Carlo method to evaluate the realizations of modal filters performance indices. For the sensors positioning uncertainties, a sampling-based sensitivity analysis is performed. Latin Hypercube Sampling technique is used to reduce the number of samples and alleviate the computational cost of analyzing multiple topologies.

2 DESIGN OF MODAL FILTERS

The design of a modal filter from an array of sensors requires the output signals of each sensor to be weighted and summed such that the response of target vibration modes is maximized while that of undesired ones are minimized. Therefore, it is possible to consider the frequency response function (FRF) of an equivalent single degree of freedom system with natural frequency ω_i and damping factor ζ_i , corresponding to the target i -th vibration mode, as the desired response of the weighted signal of the modal filter, which can be written as

$$g_i(\omega) = \frac{2\zeta_i\omega_i^2}{\omega_i^2 - \omega^2 + 2j\zeta_i\omega_i\omega}. \quad (1)$$

Whenever the vibration modes are weakly damped and relatively well spaced, the resonance peaks are well defined and, thus, (1) represents a realistic objective for the filtered FRF signal. Let \mathbf{Y} be a matrix with columns that represent the FRFs of the n selected sensors in the array and discretized in a frequency domain $[\omega_1, \dots, \omega_m]$. Let $\mathbf{G}_i = [g_i(\omega_1), \dots, g_i(\omega_m)]$ be the vector representing (1) in the discrete frequency domain. The vector of coefficients α_i which equates the filtered output (weighted sum of sensors outputs) to the one defined by the vector \mathbf{G}_i is the solution of the following system

$$\begin{bmatrix} Y_1(\omega_1) & \cdots & Y_n(\omega_1) \\ \vdots & \ddots & \vdots \\ Y_1(\omega_m) & \cdots & Y_n(\omega_m) \end{bmatrix} \begin{bmatrix} \alpha_{i1} \\ \vdots \\ \alpha_{in} \end{bmatrix} = \begin{bmatrix} g_i(\omega_1) \\ \vdots \\ g_i(\omega_m) \end{bmatrix}. \quad (2)$$

In general, the linear system defined by (2) admits only approximate solutions, which will be denoted α_i^\dagger . The vector of weighting coefficients α_i^\dagger represents the best solution, in a least squares sense, for the design of a modal filter which isolates the i -th vibration mode response. If several vibration modes are to be considered simultaneously as target modes for the filter design, it is necessary to define \mathbf{G} as the matrix of target FRFs with dimension $m \times p$, where p denotes the number of target modes. Consequently, the approximate solution of (2), α^\dagger , is a matrix of dimension $n \times p$, that is one column vector of weighting coefficients for each one of the target modes. This may be written in a compact form as

$$\mathbf{Y}\alpha^\dagger = \mathbf{G}. \quad (3)$$

Actually, $\mathbf{Y}\alpha^\dagger$ approximates \mathbf{G}^\dagger , a matrix with columns that are the orthogonal projection of the columns of \mathbf{G} onto the space spanned by the columns of \mathbf{Y} . The traditional Moore-Penrose pseudo-inverse solution of (3) for a full column rank \mathbf{Y} matrix (with columns that are linearly independent) may be obtained by pre-multiplying (3) by \mathbf{Y}^H , where the symbol H denotes the hermitian,

$$\mathbf{Y}^H\mathbf{Y}\alpha^\dagger = \mathbf{Y}^H\mathbf{G}, \quad (4)$$

such that

$$\alpha^\dagger = (\mathbf{Y}^H\mathbf{Y})^{-1}\mathbf{Y}^H\mathbf{G}. \quad (5)$$

$\mathbf{Y}^\dagger = (\mathbf{Y}^H\mathbf{Y})^{-1}\mathbf{Y}^H$ is then the pseudo-inverse of \mathbf{Y} . On the other hand, for a full column rank matrix, inversion of $\mathbf{Y}^H\mathbf{Y}$ is unnecessary and computationally inefficient, since \mathbf{Y} may be decomposed through QR decomposition, where \mathbf{Q} is an orthonormal matrix and \mathbf{R} is upper triangular, such that $\mathbf{Y} = \mathbf{Q}\mathbf{R}$ and (5) can be rewritten as

$$\alpha^\dagger = [(\mathbf{Q}\mathbf{R})^H\mathbf{Q}\mathbf{R}]^{-1}(\mathbf{Q}\mathbf{R})^H\mathbf{G}, \quad (6)$$

which, after expansion and accounting for $\mathbf{Q}^H\mathbf{Q} = \mathbf{I}$, reads

$$\alpha^\dagger = \mathbf{R}^{-1}\mathbf{Q}^H\mathbf{G}. \quad (7)$$

Notice that the inverse of \mathbf{R} does not need to be evaluated, instead the upper triangular linear system, $\mathbf{R}\alpha^\dagger = \mathbf{Q}^H\mathbf{G}$, is solved through back substitution, which is more computationally efficient. For all the cases studied in the present work, the solution through QR decomposition was always convenient, since the FRF matrix has had full column rank. If at least two columns of the FRF matrix are linearly dependent, this means that two sensors outputs are equivalent so that one of them is dispensable and the array formed by these sensors is equivalent to one with one sensor less, thus, it should present lower performance. If this is the case, the singular value decomposition (SVD) is the suitable method to approximate the least square solution.

In practice, truncation of matrix \mathbf{Y} over a given frequency range will affect its QR decomposition and, thus, the approximate solution of linear system (3). Let \mathbf{Y} be the FRF matrix truncated at frequency $\omega_t \leq \omega_m$. Recent works have shown that there is a value for $\omega_t = \omega_l$

with the SOLID226 element and the finite element meshes for both elements must be coherent.

All nodes of the piezoelectric patches surfaces bonded to the plate are considered electrically grounded. The dielectric properties of PZT-5H prevent the homogeneous distribution of the induced electrical charges on the free surface of the patches. Therefore, measurement of the electric potential in a specific node on the free surface will correspond to local information on induced strain. In practice, the upper and lower surfaces of each patch are covered with electrodes which ensure uniform induced electric potentials (equipotential).

To analyze the effect of the electrode, the mode shapes, natural frequencies and electric potential distributions for the first four vibration modes were evaluated without and with electrodes on the free surfaces of the patches. Figure 2 shows the first four vibration modes accounting for the equipotentiality condition. More details on the importance of equipotential condition on the modeling of piezoelectric structures can be found in (Trindade and Benjeddou, 2009).

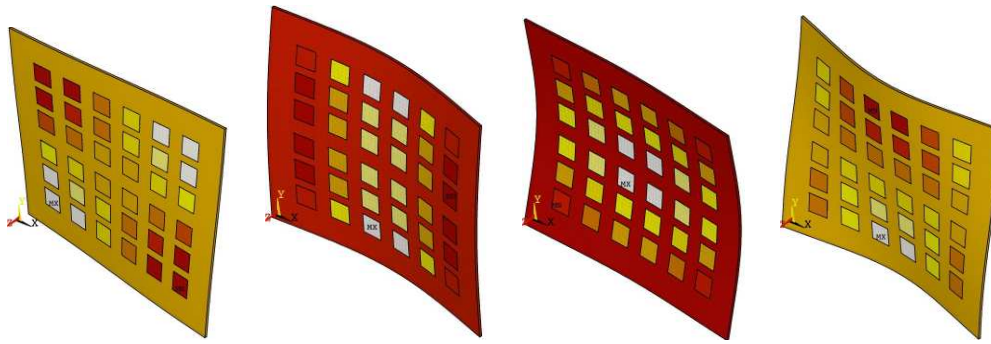


Figure 2: Mode shapes, natural frequencies and voltage distributions in the sensors for the first four vibration modes of the plate with bonded piezoceramic patches with equipotentiality condition.

3.2 Modal filter performance for a reduced number of sensors

Modal filters can be simulated and, in practice, implemented using thirty-six, or even more, sensors bonded to the aluminum plate. However, one should wish to minimize the number of sensors in the array while maximizing the performance of modal filters since using fewer sensors reduces project cost, structure weight and acquisition system complexity, which are all very important in practical applications.

Therefore, in this section, only twelve of the thirty-six sensors shown previously are considered to be active. This allows us to form a large number of reduced-dimension arrays and analyze the effect of the array topology on the performance of modal filters derived from it. It is supposed that the piezoceramic patches do not alter significantly the vibration modes and natural frequencies of the plate so that the topologies with twelve sensors may be all evaluated by simply considering the output of the selected sensors in the modal filter design. This means that the twenty-four inactive sensors are also bonded to the structure but their output is ignored. The main reason for this procedure is that most of the computational cost comes from the evaluation of the FRF matrix and, thus, in the proposed methodology this evaluation is performed only one time for the plate with thirty-six sensors, even though only twelve selected outputs will be considered for each topology. Evidently, the hypothesis that the twenty-four inactive sensors do not alter much the results shall be confirmed afterwards by remodeling the plate with only twelve sensors for given selected topologies.

The FRF of each piezoceramic patch was evaluated through modal superposition considering

the twenty-six flexible vibration modes in the frequency range [10 – 2000] Hz, with steps of 0.5 Hz, and a transversal point force applied near the upper-right corner of the plate.

Previous results indicate that, with the exception of topologies susceptible to spatial aliasing, twelve sensors should be enough for a satisfactory filtering quality in the frequency range up to 800 Hz. If it is required to increase the frequency range of the modal filters, the FRF truncation frequency for the QR decomposition could be increased but, generally, this will lead to a loss in the filtering quality. One could also think of increasing the number of sensors in the array to increase the frequency range of the modal filters derived from it. This was done here by considering the average and standard deviation of a sample of 10^4 arbitrary topologies with sixteen sensors, selected from the thirty-six of the base array. 10^4 arbitrary topologies with twelve sensors are considered for comparison purposes. The FRFs considered for the QR decomposition are truncated at 1000 Hz, which leads to a frequency range containing fourteen vibration modes. Figure 3 shows the average and one standard deviation confidence interval output of modal filters designed to isolate the first vibration mode using twelve and sixteen sensors. For sixteen sensors, the modal filter is very effective in isolating the first resonance for any of the 10^4 arbitrary topologies considered, since the standard deviation of the response nearly vanishes up to 1000 Hz (Figure 3b). For twelve sensors, unfiltered residual response for other resonances in the frequency range of interest can be observed (Figure 3a). However, based on the one standard deviation confidence intervals, it is possible to assume that there may be some specific topologies of twelve sensors that lead to effective modal filters.

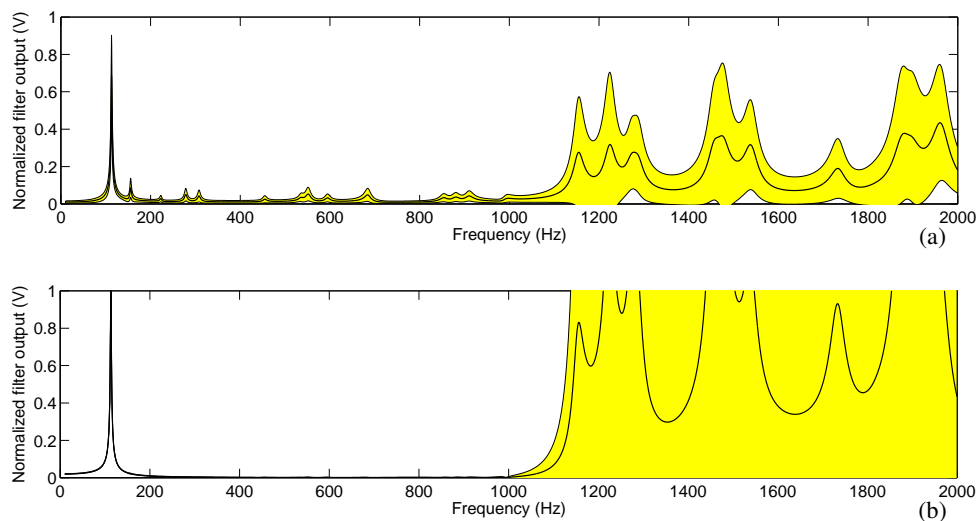


Figure 3: Average and one standard deviation confidence interval of the output of first mode modal filters based on a sample of 10^4 arbitrary topologies of twelve (a) and sixteen (b) sensors.

The analyses presented in this section indicate that although, in average, the number of modes, and thus the frequency range of the modal filter, is limited by the number of sensors considered, properly selected topologies could increase the frequency range, for a given number of sensors, or reduce the number of sensors, for a given frequency range. This suggests that the topology of an array of sensors could be optimized to enhance its performance.

4 OPTIMIZATION OF THE SENSORS ARRAYS TOPOLOGIES

This section presents a methodology for improving filtering performance through the optimization of the sensors arrays topologies.

4.1 Optimization strategy

After some numerical simulations with straightforward topologies derived from the base array with thirty-six sensors, it becomes clear that the relation between the array topology and the filtering performance is quite complex, even when the mode shapes are known, and, hence, optimal solutions require a more advanced strategy. An extensive search of the possible combinations of twelve sensors from the thirty-six available would lead to an impracticable computational cost, since around one billion ($C_{36,12}$) combinations would have to be evaluated. Extensive search could however be considered using selected subspaces to identify rationales for the parameters' setup of another search strategy (Pagani and Trindade, 2008b).

GAs are more suitable search methods in these cases when the research space is too large, strongly multimodal and non-linear. It is chosen here to setup a GA search by defining a random initial population formed by so-called individuals with chromosomes that are composed of twelve genes. Each gene is an integer number from 1 to 36 representing the sensor index. Therefore, one individual represents a sensors array topology formed by the twelve sensors defined by its genes.

Following the standard GA evolutive process, the initial population is considered to evolve along a set of generations through reproduction (crossover), mutation and selection operations. While reproduction and mutation operations aim to provide diversity to the population, the selection operation aims to rank individuals with respect to a fitness or objective function. Since this is a random search algorithm, the optimal results are dependent on the initial population and on the reproduction, mutation and selection parameters. However, it is expected that for a sufficiently large number of generations or size of the initial population, the algorithm will converge to the global optimum. More details on convergence and selection of operations parameters can be found in (Pagani and Trindade, 2008b).

Since any individual of the population is composed by twelve different integer numbers in the domain $[1, \dots, 36]$, a specific routine was written to build the initial population. For each individual, the routine scrambles randomly a vector of integers from 1 to 36 and, then, the first 12 elements of the scrambled vector define the corresponding individual. This procedure is repeated for all individuals in the initial population. The selection of the first 12 elements in the scrambled vector does not imply in a tendency since the distribution of the sensor indices in the vector is equiprobable.

The mutation operation, considered in this work, consists in replacing one of the 12 genes (sensors), selected randomly, of an individual by another one, selected randomly from the complementary group of sensors, that is, from the 24 remaining sensors not present in the individual. This procedure prevents the generation of an individual with repeated genes. The reproduction (crossover) operation combines the initial and final sections of two individuals (parents) to form a new individual (child), where the breaking position of the parents' sequences (chromosomes) is defined randomly. In this case, the generation of an individual with repeated genes is possible and, when this is the case, the fitness function of this individual is not evaluated to save computational time; instead a small fitness value is attributed to it, such that its selection probability is also small. The selection operation is based on a stochastic universal sampling algorithm, where the expectation of individuals in the population is evaluated from a fitness ranking.

Besides the choice of reproduction, mutation and selection operators, it is necessary to define the size of the initial population (N), the number of best individuals (elite) which are kept unmodified from one generation to another (Σ), the percentage of the population in each generation which are generated by crossover (T_c) and the total number of generations the population evolves (N_p). Once defined T_c , the remaining part of population is generated by either the previous elite or mutation operation. Crossover percentages of [30, 40, 50, 60, 70]% lead to genic mutation rates of [5.8, 5.0, 4.2, 3.3, 2.5]%. Apart from the procedures proposed for the construction of the initial populations, the mutation operation and the parameters' definition, the optimization was performed using operators and algorithms of MATLAB Genetic Algorithm and Direct Search (GADS) Toolbox.

4.2 Objective function to rank the modal filters performance

The objective of the present optimization is to find the topology of an array with twelve sensors that maximizes the filtering quality, over a given frequency range, of modal filters designed to isolate a given set of resonances of the structure. In the present work, a particular case of interest was studied using the first three vibration modes of the free plate as target vibration modes to be isolate by the modal filters. The target frequency range is [0, 1000] Hz, which is higher than the limit frequency $\omega_l = 800$ Hz for the present case and contains fourteen resonances (four after ω_l). Therefore, the FRF truncation frequency is defined as $\omega_t = 1000$ Hz such that, for an arbitrary array topology, no filtering quality can be guaranteed along the frequency range, while an optimal topology can maximize this quality. For implementation purposes, the objective function to be minimized is then defined as the residual error norm

$$J = \left\| \mathbf{G}_t - \mathbf{Y}_t \boldsymbol{\alpha}^\dagger \right\|_2. \quad (8)$$

where \mathbf{G}_t and \mathbf{Y}_t are the target and measured, by each sensor, FRFs truncated at frequency ω_t and $\boldsymbol{\alpha}^\dagger$ is the vector of weighting coefficients, evaluated using \mathbf{G}_t and the QR decomposition of matrix \mathbf{Y}_t in (7).

Another possible strategy that was presented in a previous work consists on maximizing the frequency range for a given filtering quality (Pagani and Trindade, 2008a).

4.3 Results for the optimal topology

In this section, the results obtained for the modal filters with optimal sensors array topologies are presented. Based on previous studies (Pagani and Trindade, 2008b), the following parameters were set for the GA optimization: initial population of $N = 1500$ individuals, crossover rate at $T_c = 45\%$, genic mutation rate at $T_g = 4.6\%$, elite population at $\Sigma = 2$ individuals and termination criteria at $N_p = 35$ generations. To minimize the dependence of GA optimization on the initial population, fifty simulations with different initial populations were performed for each case and the best results from these simulations are saved.

Figure 4 presents the normalized filters outputs, such that the amplitude at target resonances is unitary, and the corresponding optimal topology, in which the twelve selected sensors are highlighted from the original thirty-six sensors array. It shows that topology optimization for isolation of the first two vibration modes has provided excellent performance up to 1000 Hz. Therefore, the modal filter was effective up to the fourteenth mode and, thus, four additional resonant modes were effectively filtered compared to an arbitrary topology. Figure 4 also shows the normalized filters output when only the real part of the weighting coefficients are considered. This verification is important because it is much easier to implement in practice a weighted sum

circuit if the weighting coefficients are all real. It can be noticed that neglecting the imaginary part of the weighting coefficients does not affect significantly the quality of the filters.

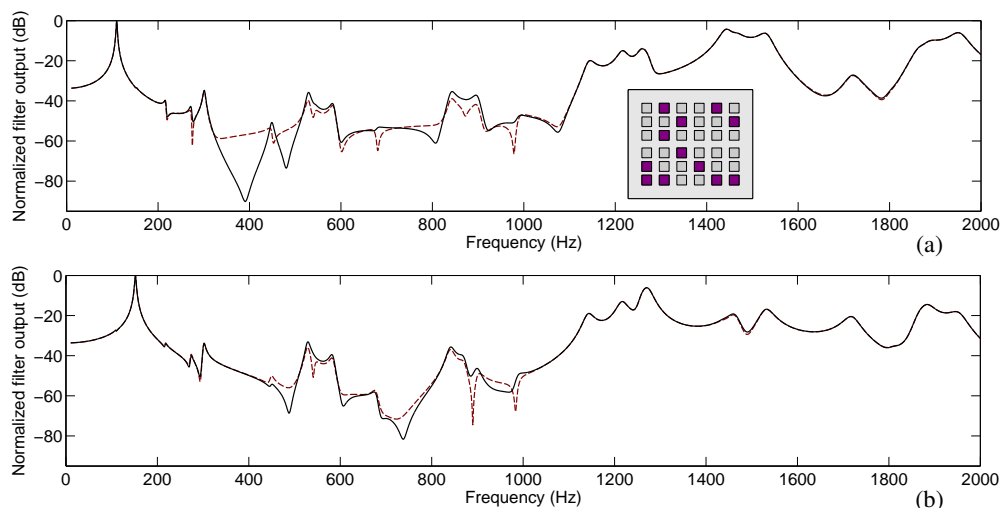


Figure 4: Normalized outputs of the modal filters designed for the isolation of first (a) and second (b) vibration modes with real (solid) and complex (dashed) weighting coefficients.

As it was shown, it is possible to improve the effectiveness and frequency-band of a set of modal filters with a reduced number of sensors by optimizing the topology of the sensor array. However, this optimization may also lead to a higher sensitivity of modal filters performance on design parameters. Therefore, the next section presents a robustness analysis of these modal filters using an optimal topology subjected to uncertainties in the weighting coefficients and in the sensors positioning.

5 UNCERTAINTIES ANALYSIS

5.1 Effect of weighting uncertainties

This section presents an approach for analyzing random uncertainties in the weighting coefficients. A Gaussian probability density function is assumed for each weighting coefficient α_j , for which the mean values are based on the nominal ones designed in the previous section and the standard deviations are estimated from experiments, such that

$$p(\alpha_j) = \frac{1}{\sqrt{2\pi}\sigma_\alpha} \exp\left\{-\frac{1}{2\sigma_\alpha^2}(\alpha_j - \bar{\alpha}_j)^2\right\} \quad (9)$$

where $\bar{\alpha}_j$ are the real part of the weighting coefficients, normalized to the maximum weight of 0.35 allowed by the voltage divider circuit used for the measurements. σ_α is an estimation of the standard deviation based on 12 sample experiments, each consisting of a manual setup of the potentiometer in one of the 16 similar circuits constructed in the laboratory. Since the level of precision in the manual setup is much more dependent on the sensibility of each potentiometer, the measurement technique for setup verification and the user's experience, than the nominal value of the weighting coefficient, the standard deviation σ_α was considered to be constant for all weighting coefficients. Based on laboratory experiments, the value of σ_α was set to 0.0003.

Based on these assumptions, N random realizations were generated for each weighting coefficient with MATLAB function *normrnd* and, then, combined to form N random realizations

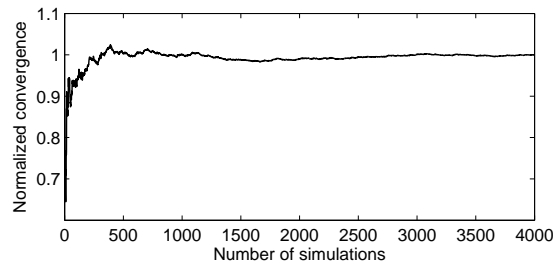


Figure 5: Mean square convergence of Monte Carlo simulation using $\sigma_\alpha = 0.0003$.

of the vector of weighting coefficients $\alpha(\theta_i)$. Each realization $\alpha(\theta_i)$ was then used to evaluate a realization of the filter output $\tilde{\mathbf{G}}(\theta_i) = \mathbf{Y}\alpha(\theta_i)$. The mean-square convergence analysis with respect to the independent realizations $\tilde{\mathbf{G}}(\theta_i)$ was carried out considering the function

$$conv(n_s) = \frac{1}{n_s} \sum_{i=1}^{n_s} \|\tilde{\mathbf{G}}(\theta_i) - \tilde{\mathbf{G}}^N\|^2, \quad (10)$$

where n_s is the number of simulations, or the number of sets of weighting coefficients considered, and $\tilde{\mathbf{G}}^N$ is the response calculated using the corresponding mean model. Figure 5 shows the mean-square convergence analysis. It is possible to observe that 2000 simulations are enough to assure convergence. Despite that, the statistical analyses presented in the following sections consider all $N = 4000$ simulations performed.

The statistical analyses of the FRFs were performed from a Gamma distribution fit to their amplitudes at each frequency to calculate maximum likelihood estimates of the distribution parameters using MATLAB function *gamfit*. Then, these parameters were used to calculate the 95% confidence intervals for the FRF amplitudes, with MATLAB function *gaminv*. More details on the stochastic modeling methodology used here can be found in (Cataldo et al., 2009; Soize, 2001; Santos and Trindade, 2009).

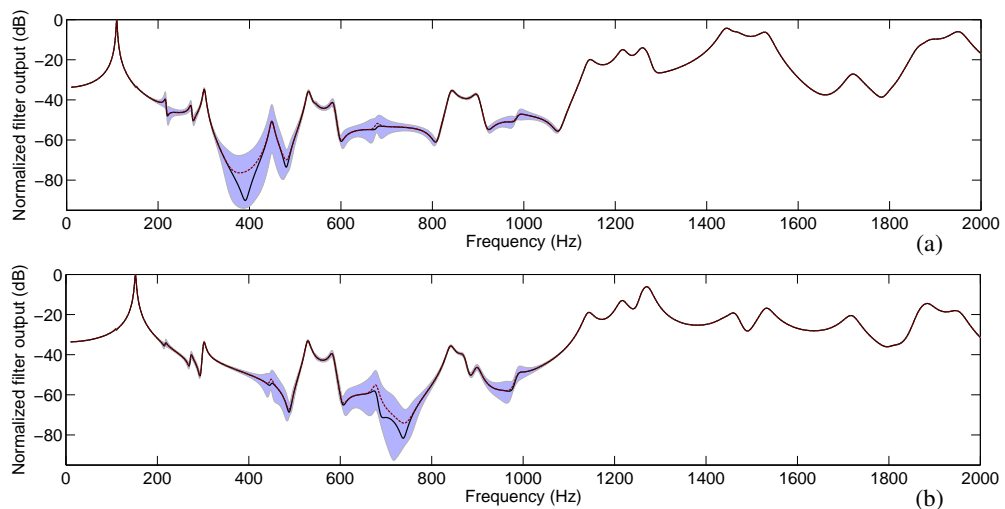


Figure 6: Nominal values (solid), mean values (dashed) and 95% confidence intervals (area) for the normalized outputs of the modal filters designed for the isolation of first (a) and second (b) vibration modes.

Figures 6 shows the normalized filter outputs when using the gaussian model for α and when

using the nominal model (nominal α). The normalized filter output using the gaussian model for the weighting coefficients vector is represented by its mean value and 95% confidence interval. From Figure 6, it is possible to notice that the uncertainty in the weighting coefficients may yield variations in comparison with the nominal model of the order of 6% for the value considered for the standard deviation σ_α .

5.2 Effect of positioning uncertainties

This section presents an analysis of the effect of random uncertainties on the positioning of the twelve sensors of the optimal topology presented previously. As discussed previously, topology optimization allows to use less sensors than it would be necessary otherwise for the design of modal filters. However, modal filters based on such optimal arrays of sensors become sensitive to the sensors positioning. Therefore, it is important to quantify the sensitiveness of a given optimal topology to perturbations on the positioning of its sensors. Instead of using local methods, such as gradient-based methods, to perform a sensitivity analysis, here a sampling-based analysis is used (Helton et al., 2006). This is much more complicate than the previous analysis of weighting coefficients since, for each perturbation in a given sensor positioning, the dynamic stiffness of the structure is modified and, thus, a new structural model should be constructed and used to evaluate the voltage frequency responses of all sensors in the array. This fact not only leads to higher computational cost, due to multiple evaluations of the structural harmonic response, but also requires special attention to whether the changes in output are due to perturbations in sensors positioning or to the reconstruction of structural model.

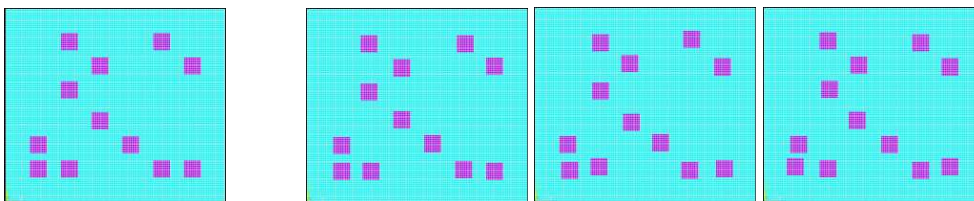


Figure 7: Optimal topology for the isolation of the first two vibration modes and three of its arbitrary perturbations.

The methodology used in this work to prevent variability due to structural modeling was to consider a fixed finite element mesh over which the piezoelectric sensors can be repositioned. The finite element model presented previously can be used but only allows positioning perturbations in steps of 5 mm, which is the mesh refinement. Therefore, a second finite element model similar to the previous one but with a mesh refinement of 2.5 mm was built. In this case, for the plate, 14336 (128 x 112) SHELL99 elements were used, while 200 SOLID226 elements were considered for each piezoceramic patch. It is unnecessary to state that this increases heavily the computational cost of one harmonic analysis in ANSYS, as compared to the coarser mesh model. Figure 7 shows the optimal topology together with the finite element mesh considered and three of the one hundred perturbed topologies used in the present analysis. The one hundred perturbed topologies were obtained using Latin Hypercube Sampling (LHS), which is an interesting method when the number of samples is relatively small and consists on maximizing the distance between the samples. Since the positioning perturbation must be performed in steps of 2.5 mm, two vectors of displacements in x and y directions relative to the optimal position, $\Delta x \in \{-1, 0, 1\}$ and $\Delta y \in \{-1, 0, 1\}$, were constructed for each piezoelectric sensor. This leads to a vector of 24 elements with values in $\{-1, 0, 1\}$ defining the perturbed topology described by the displacements along x and y directions of each piezoelectric sensor relative to

its optimal position. Then, the LHS technique was used to construct one hundred samples of the 24 elements vector.

For each perturbed topology, the FRF was evaluated for each one of the twelve piezoelectric sensors and, then, used to evaluate the modal filters output responses through multiplication by the real part of the optimal (unperturbed) vector of weighting coefficients, $\bar{\alpha}$. The results for the first and second modes modal filters output are shown in Figure 8 for all perturbed topologies. A large variation of the filter output response can be noted inside the frequency range of interest in which the response should be filtered.

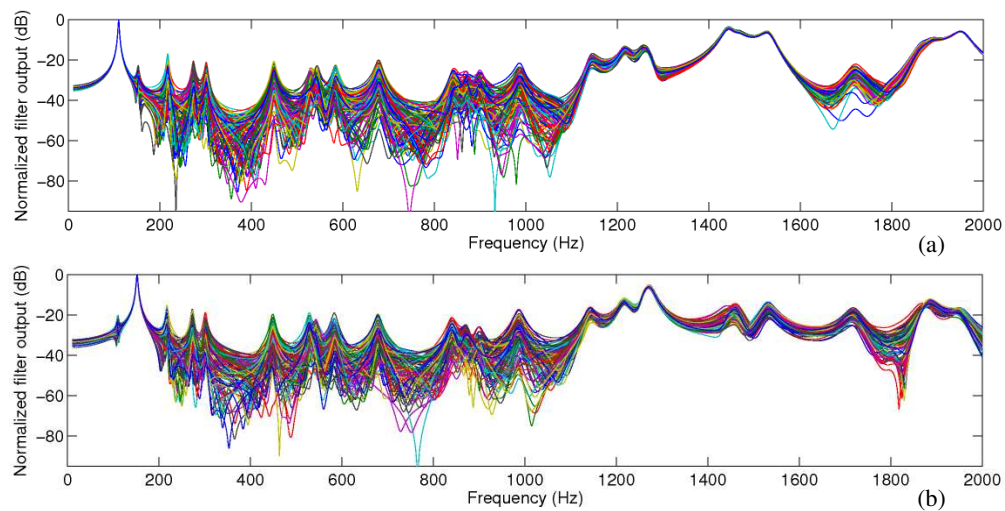


Figure 8: Normalized filter outputs for first (a) and second (b) modes obtained using the perturbed topologies using displacement steps of 2.5 mm.

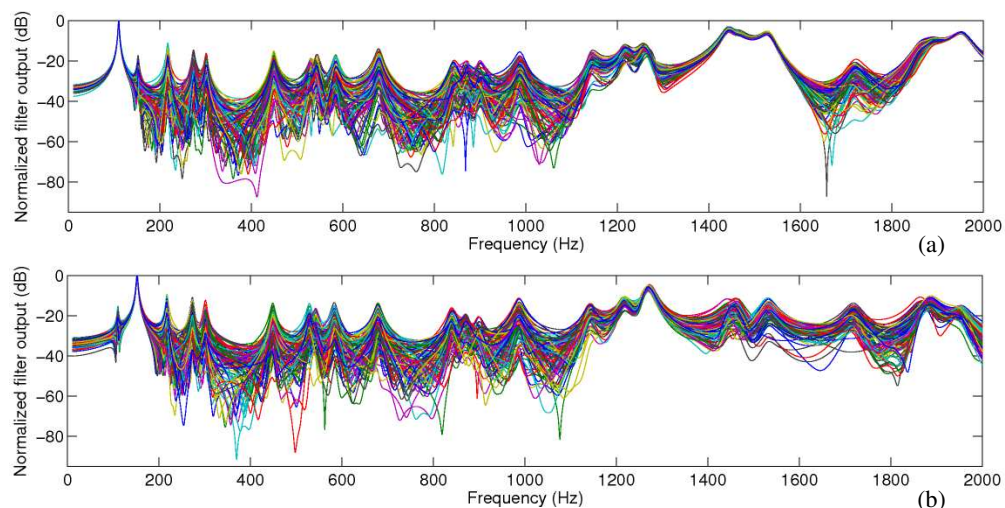


Figure 9: Normalized filter outputs for first (a) and second (b) modes obtained using the perturbed topologies using displacement steps of 5 mm.

To save computational effort, the same analysis was performed for higher (5 mm) displacement steps using the finite element model with coarser mesh (5 mm mesh refinement). The

results are presented in Figure 9. Although it is not presented here, a comparison between the unperturbed responses using the 2.5 mm and 5 mm spaced meshes was made and found to have no significant effect on the evaluation of the modal filters output responses. Therefore, the unperturbed response using the finer mesh (2.5 mm) can be used as reference to the perturbed responses with displacement steps of 5 mm.

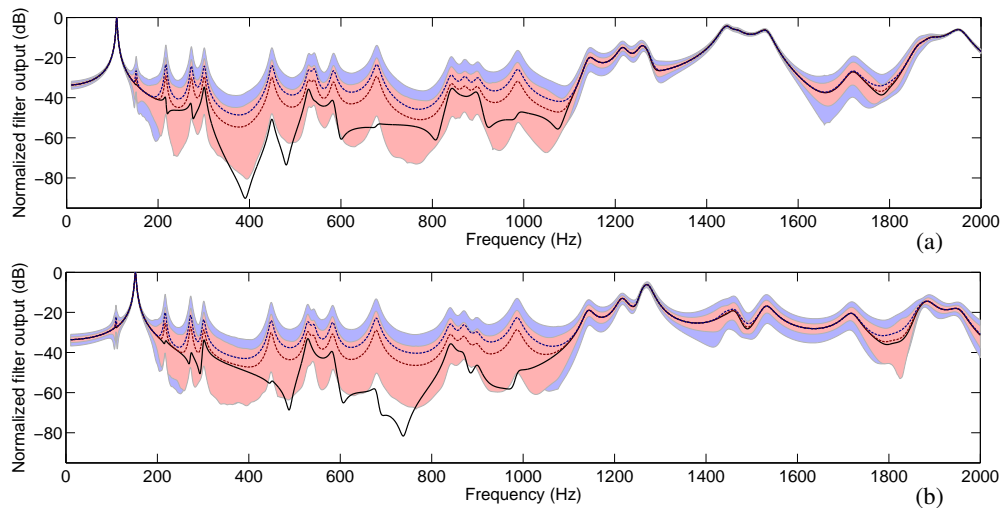


Figure 10: Mean and 95% confidence interval of the normalized first (a) and second (b) modes filters outputs compared to the unperturbed (black) output for 2.5 mm (red) and 5 mm (blue) displacement steps.

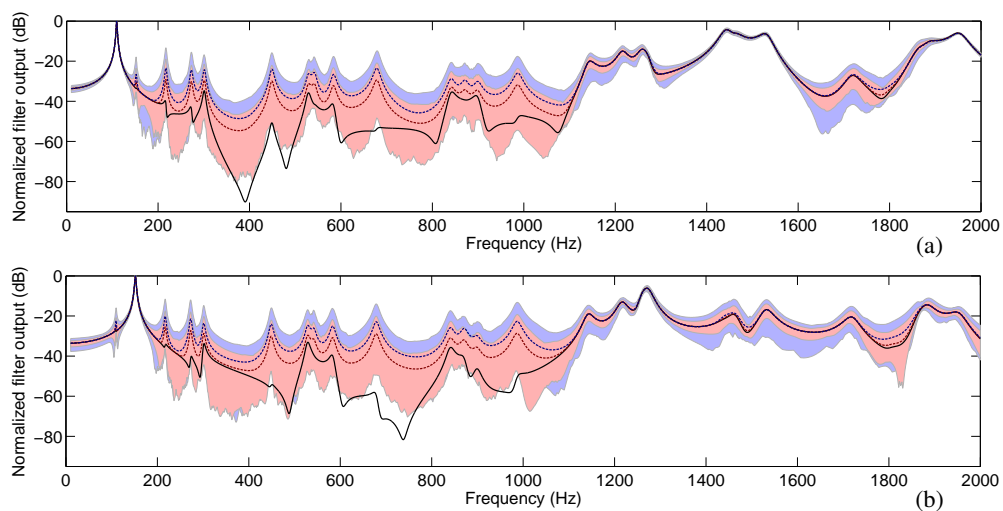


Figure 11: Mean and 2.5-97.5% percentiles interval of the normalized first (a) and second (b) modes filters outputs compared to the unperturbed (black) output for 2.5 mm (red) and 5 mm (blue) displacement steps.

Then, two methodologies were considered to quantify the filtering quality decrease due to the topology perturbations. First, the distribution of filter output amplitudes, for each frequency point, was fitted into a Gamma probability distribution function which was then used to evaluate the 95% confidence interval of the distribution. The results for both first and second modes modal filters and for smaller (2.5 mm) and larger (5 mm) displacement steps are presented in

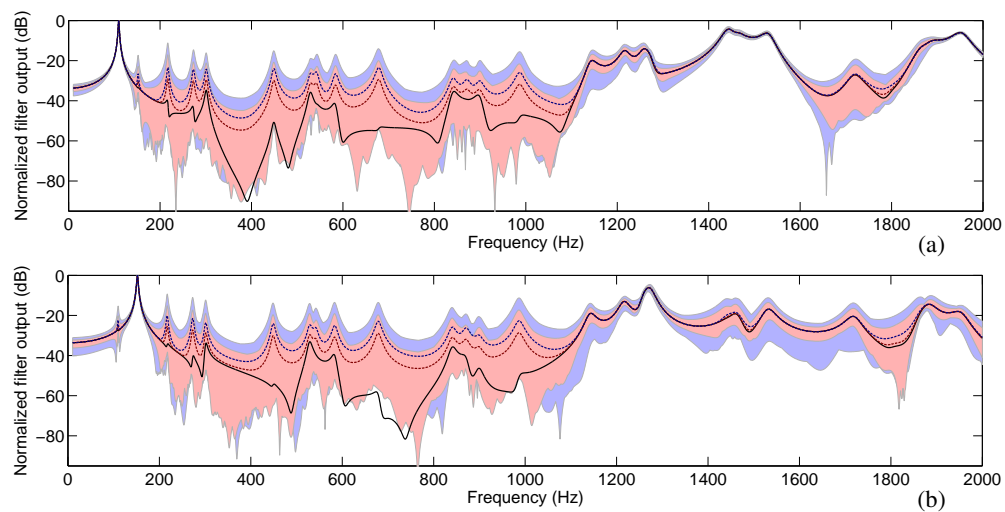


Figure 12: Mean and minmax interval of the normalized first (a) and second (b) modes filters outputs compared to the unperturbed (black) output for 2.5 mm (red) and 5 mm (blue) displacement steps.

Figure 10. It can be noticed that the responses differ mainly inside the frequency range of interest. As expected, smaller values for the perturbation (displacement) steps lead to better filtering quality. It can also be observed that the perturbation yields a mean output for which the amplitude of the filtered resonances are set to the same order of magnitude. This suggests that the perturbation decreases the filtering quality more for the resonances that are better filtered. From the 95% confidence interval, the maximum error for the first mode modal filter is approximately 20%, for a 5 mm perturbation, and 10%, for a 2.5 mm perturbation. For the second mode modal filter, these maximum errors are, respectively, 28% and 13%. The maximum error is located at the third resonance for all cases. Although, it is not advisable to interpolate these results to estimate the confidence interval for other perturbation magnitudes, it is reasonable to guess that perturbations smaller than 2.5 mm should lead to errors smaller than 10%. Considering the mean outputs, the maximum errors for the first and second modes modal filters are, respectively, 6.7% and 10% for larger perturbation and 3.5% and 5.5% for smaller perturbation. The average filtering errors for the first and second modes modal filters over the frequency range of interest (200-1000 Hz) are, respectively, 2% and 2.5% for larger perturbation and 1% and 1.3% for smaller perturbation.

Since there is no guarantee that the distribution of filter output amplitudes is well fitted by a Gamma probability distribution function, a second methodology was considered to quantify the loss of filtering quality due to the topology perturbation. Figure 11 shows the confidence intervals evaluated using the 2.5-97.5% percentiles. It can be noticed that Figures 10 and 11 are very similar, apart from a less smooth lower interval for the latter. In terms of maximum filtering errors, results similar to the previous ones are also obtained, 21% and 26% for larger perturbation and 11% and 13% for smaller perturbation.

Another methodology that could be used is to consider the full intervals from the samples considered, i.e. maximum and minimum amplitudes obtained for the filter outputs. These are shown in Figure 12. As expected, the intervals become wider and with less smooth lower interval. The maximum filtering errors obtained using this methodology are 27% and 34% for larger perturbation and 14% and 17% for smaller perturbation.

6 CONCLUSIONS

This work presented a robustness analysis of modal filters using a topology optimized array design with a reduced number of sensors subjected to uncertainties in the weighting coefficients and sensors positioning. For the weighting coefficients uncertainties, this was done using stochastic modeling tools to build a probabilistic model of the uncertain parameters and Monte Carlo method to evaluate the realizations of modal filters performance indices. It was shown that optimal filter output is somewhat sensitive to the weighting coefficients but, as long as the standard deviation from nominal values are kept around 0.0003, the performance predicted with the nominal model is satisfactorily reliable. For the sensors positioning uncertainties, a sampling-based sensitivity analysis was performed. Latin Hypercube Sampling technique was used to reduce the number of samples and alleviate the computational cost of analyzing multiple topologies. It was shown that for perturbation displacements smaller than 2.5 mm, the filtering error should be smaller than 10% approximately. Future works will include experimental validation of these uncertainties analyses and applications for active vibration control.

ACKNOWLEDGEMENTS

The authors acknowledge the support of the MCT/CNPq/FAPEMIG National Institute of Science and Technology on Smart Structures in Engineering, grant no.574001/2008-5. The second author also acknowledges CAPES for a graduate scholarship.

REFERENCES

- Cataldo, E., Soize, C., Sampaio, R. and Desceliers, C. Probabilistic modeling of a nonlinear dynamical system used for producing voice. *Computational Mechanics*, 43:265–275, 2009.
- Chen, C.Q. and Shen, Y.P. Optimal control of active structures with piezoelectric modal sensors and actuators, *Smart Materials and Structures*, 6:403–409, 1997.
- Chopra, I. Review of state of art of smart structures and integrated systems, *AIAA Journal*, 40:2145–2187, 2002.
- Frecker, M.I. Recent advances in optimization of smart structures and actuators, *Journal of Intelligent Material Systems and Structures*, 14:207–216, 2003.
- Fripp, M.L. and Atalla, M.J. Review of modal sensing and actuation techniques, *The Shock and Vibration Digest*, 33:3–14, 2001.
- Friswell, M. On the design of modal actuators and sensors, *Journal of Sound and Vibration*, 241:361–372, 2001.
- Goldberg, D. *Genetic algorithms in search, optimization, and machine learning*, Addison-Wesley Pub. Co., 1989.
- Han, J.-H. and Lee, I., Optimal placement of piezoelectric sensors and actuators for vibration control of a composite plate using genetic algorithms, *Smart Materials and Structures*, 8(2):257–267, 1999.
- Helton, J.C., Johnson, J.D., Sallaberry, C.J., and Storlie, C.B. Survey of sampling-based methods for uncertainty and sensitivity analysis, *Reliability Engineering and System Safety*, 91:1175–1209, 2006.

- Meirovitch, L. and Baruh, H. Control of self-adjoint distributed-parameter systems, *AIAA Journal of Guidance, Control and Dynamics*, 5(1):60–66, 1982.
- Pagani Jr., C.C. and Trindade, M.A. Projeto e otimização do desempenho de filtros modais baseados em redes de sensores piezoelétricos, *Proceedings of 7o Simpósio de Mecânica Computacional*, Belo Horizonte, ABMEC, 2008a.
- Pagani Jr., C.C. and Trindade, M.A. Otimização topológica de redes de sensores piezoelétricos para o projeto de filtros modais, *Proceedings of 29th Iberian Latin American Congress on Computational Methods in Engineering*, 2008b.
- Pagani Jr., C.C. and Trindade, M.A. Optimization of modal filters based on arrays of piezo-electric sensors, *Smart Materials and Structures*, 18:095046, 2009.
- Preumont, A., François, A., De Man, P. and Piefort, V. Spatial filters in structural control, *Journal of Sound and Vibration*, 265:61–79, 2003.
- Santos, H.F.L. and Trindade, M.A. Vibration control using extension and shear active-passive piezoelectric networks subject to parametric uncertainties, *Proceedings of the XIII International Symposium on Dynamic Problems of Mechanics (DINAME)*, 2009.
- Shelley, S.J. *Investigation of Discrete Modal Filters for Structural Dynamic Applications*, Ph.D. Thesis, University of Cincinnati, 1991.
- Soize, C. Maximum entropy approach for modeling random uncertainties in transient elastodynamics, *Journal of the Acoustical Society of America*, 109(5):1979–1996, 2001.
- Trindade, M.A. Optimization of active-passive damping treatments using piezoelectric and viscoelastic materials, *Smart Materials and Structures*, 16(6):2159–2168, 2007.
- Trindade, M.A. and Benjeddou, A. Effective electromechanical coupling coefficients of piezo-electric adaptive structures: critical evaluation and optimization, *Mechanics of Advanced Materials and Structures*, 16(3):210–223, 2009.